

Conclusion

Based on the recent research results on the properties of Dielectric Resonators it became obvious that their potential capabilities have not been fully discovered. The interested reader can simply find a significant number of publications on the analysis of new DR properties in the microwave and infrared wavelength ranges. The special interest arises in a deep analogy, noticed in a lot of publications, regarding the similarity in behavior of coupled DR system and the properties of the molecules and crystals. The scattering of electromagnetic waves on the DR systems in Open space also adduces reasons in support of the conception about existence of profound relations between electrodynamics and the scattering quantum theory. Herewith, the DR lattices often demonstrate interesting frequency-selective properties, lacking in the continuous media. All in all, it is fair to say that the coupled DR systems present one more interesting area of modern physics, located on the edge of classical and quantum theory.

Notably, the author intentionally does not focus on the possible areas of DR lattices' application. Today their properties have been extensively explored in different laboratories. Obviously, the practical usage of the DR lattices will lead to significant improvements in different devices of microwave, infrared, and optical wavelength ranges. Their resonance properties allow the substantial improvement of coupling provision with electromagnetic field. Hence, by analyzing their properties more effective novel devices for information manipulation and storage in the infrared and optical ranges can be proposed and manufactured.

Appendix 1

The Fields of the DR Eigenmodes in the Open Space

Let us consider eigenoscillations of the homogeneous Spherical DR with relative dielectric permittivity ϵ_{1r} in the Open space (Fig. A.1a). In the general case the solutions to the Maxwell's equations in the spherical coordinate system can be divided into the magnetic and electrical types:

For the magnetic type the field describes by equals zero of the radial electrical component. This type is denoted by H_{nml}

$$\begin{aligned}
 e_r &= 0; \\
 e_\theta &= -i\omega\mu_0 f_n^{(s)}(k_s r) m \frac{P_n^m(\cos \theta)}{\sin \theta} \begin{bmatrix} \cos & \\ -\sin & m\varphi \end{bmatrix}; \\
 e_\varphi &= i\omega\mu_0 f_n^{(s)}(k_s r) \frac{dP_n^m(\cos \theta)}{d\theta} \begin{bmatrix} \sin & \\ \cos & m\varphi \end{bmatrix}; \\
 h_r &= \frac{n(n+1)}{r} f_n^{(s)}(k_s r) P_n^m(\cos \theta) \begin{bmatrix} \sin & \\ \cos & m\varphi \end{bmatrix}; \\
 h_\theta &= \frac{1}{r} \frac{d}{dr} \left\{ r f_n^{(s)}(k_s r) \right\} \frac{dP_n^m(\cos \theta)}{d\theta} \begin{bmatrix} \sin & \\ \cos & m\varphi \end{bmatrix}; \\
 h_\varphi &= \frac{1}{r} \frac{d}{dr} \left\{ r f_n^{(s)}(k_s r) \right\} m \frac{P_n^m(\cos \theta)}{\sin \theta} \begin{bmatrix} \cos & \\ -\sin & m\varphi \end{bmatrix}.
 \end{aligned}
 \tag{A.1.1}$$

The second type describes by equals zero of the radial magnetic component $h_r = 0$. This type, named the electric is labelled as E_{nml} . The corresponding components of the electric type can be found from (A.1.1) with the help of the replacement $\vec{e} \rightleftharpoons \vec{h}$ and $\mu_0 \rightleftharpoons -\epsilon_s$.

Here $P_n^m(\cos \theta)$ —is the associated Legendre polynomial; $f_n^{(s)}(z)$ —one of the spherical Bessel functions [2]: $j_n(z) = (\pi/2z)^{1/2} J_{n+1/2}(z)$; $y_n(z) = (\pi/2z)^{1/2} Y_{n+1/2}(z)$; $h_n^{(2)}(z) = (\pi/2z)^{1/2} H_{n+1/2}^{(2)}(z)$, or their linear combinations. In our case

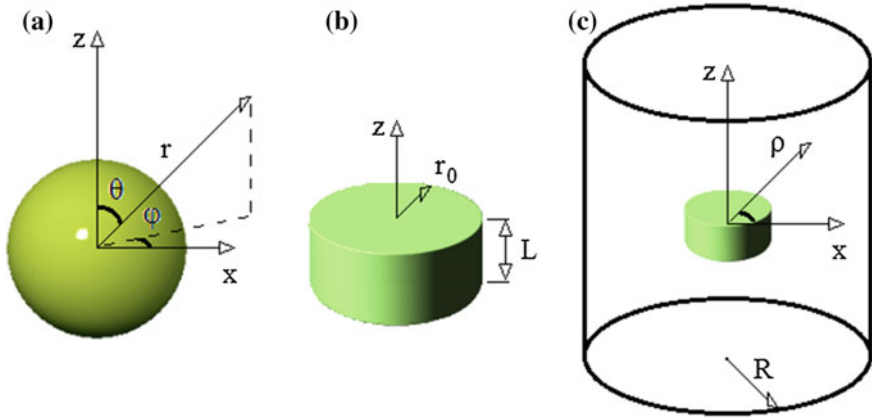


Fig. A.1 The spherical DR (a). The cylindrical DR in the open space (b). The cylindrical DR in the circular cylindrical waveguide (c)

the indexes n ; $|m| \leq n$ are integer and determine the number of field variations in the meridional plane: $\varphi = \text{const}$ and on the surface: $\theta = \text{const}$, respectively.

Inside the dielectric sphere in Fig. A.1a ($r \leq r_0$, here r_0 —is the radius of the resonator) the solution should meet the requirement of the finiteness of field at the origin of the coordinate system ($r = 0$): $f_n^{(1)}(k_1 r) = a_1 j_n(k_1 r)$. In the external space ($r > r_0$), starting from the radiation condition, one obtains $f_n^{(0)}(k_0 r) = a_0 h_n^{(2)}(k_0 r)$. Here $k_0 = \omega \sqrt{\mu_0 \varepsilon_0}$, $k_1 = \omega \sqrt{\mu_0 \varepsilon_1}$ —are the wave numbers; a_0 , a_1 —are the unknown amplitudes; ω —is the circular frequency; μ_0 —is the magnetic permeability; ε_0 ; ε_1 —is the dielectric permittivity of the external space and dielectric sphere, respectively.

By satisfying the continuity condition of the field's tangent components on the dielectric surface ($r = r_0$) the following relations have been derived:

For the magnetic modes H_{nml} :

$$a_1 = h_1; \quad a_0 = \frac{j_n(p)}{h_n^{(2)}(q)} h_1; \quad (\text{A.1.2})$$

For the electrical modes E_{nml} :

$$a_1 = e_1; \quad a_0 = \varepsilon_1 r \frac{j_n(p)}{h_n^{(2)}(q)} e_1. \quad (\text{A.1.3})$$

Below, the nondimensional numbers $p = k_1 r_0$, $q = k_0 r_0$ will be named as characteristic parameters of the Spherical DR.

The nontrivial solutions (A.1.2) and (A.1.3) exist, if the characteristic parameters p , q satisfy equations [3]

$$\varepsilon_{1r}^{-1/2} j_n(p) h_{n-1}^{(2)}(q) = j_{n-1}(p) h_n^{(2)}(q) \quad (\text{A.1.4})$$

for the magnetic modes H_{nml} , and

$$\varepsilon_{1r}^{-1} \frac{d}{dp} \{p j_n(p)\} h_n^{(2)}(q) = j_n(p) \frac{d}{dq} \{q h_n^{(2)}(q)\} \quad (\text{A.1.5})$$

for the electrical modes E_{nml} .

By applying the numerical methods toward the characteristic equations (A.1.4) and (A.1.5) the complex solutions can be obtained, corresponding to the eigenoscillation modes of Spherical DR. Below, via l the number of radial root of (A.1.4) or (A.1.5) has been denoted. The real part of the characteristic parameter: $p_R = \text{Re } p$ defines the frequency of the mode, while the imaginary part: $p_J = \text{Im } p$ defines losses, associated with radiation and dielectric dissipation. Q-factor of the mode can be calculated according to the formula: $Q_\Sigma = p_R / 2p_J$.

The lowest resonance frequency of the resonance corresponds to the main magnetic mode, namely H_{1m1} . The field of the mode is similar to the field of the magnetic dipole (Fig. A.2a).

As for higher oscillation modes, at present the maximal interest arises in the whispering gallery modes, for which $n \gg l$ is true. The modes with different values of $|m| \leq n$ indexes are called degenerate, since they have equal resonance frequencies. The main feature of the whispering gallery modes is that their fields concentrate in the area of dielectric-air surface. The examples of several field distributions of the Spherical DR operating in whispering gallery modes have been shown in Fig. A.3.

For Cylindrical DRs (Fig. A.1b), an accurate single-wave solution to the eigenoscillation problem, satisfying the continuity and radiation conditions, does

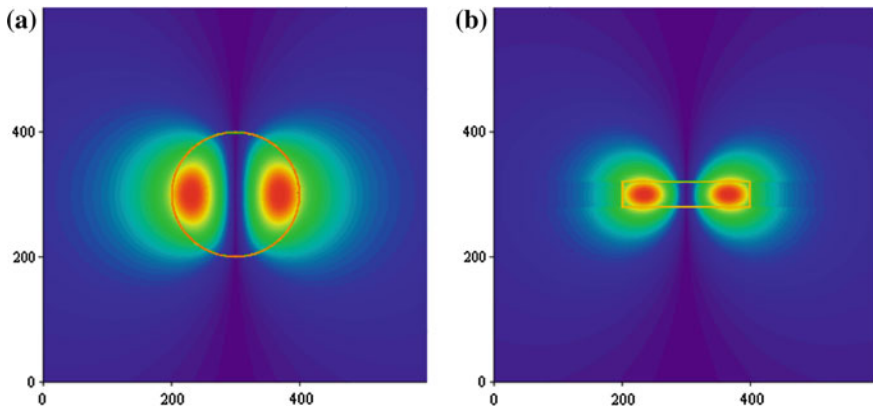


Fig. A.2 Electric field distribution of the H_{101} mode of the Spherical DR (a) ($\varepsilon_{1r} = 16$); of the cylindrical H_{101}^+ mode ($\varepsilon_{1r} = 36$; $\Delta = 0, 2$) DR (b) in the plane: $\varphi = c$; $c + \pi$

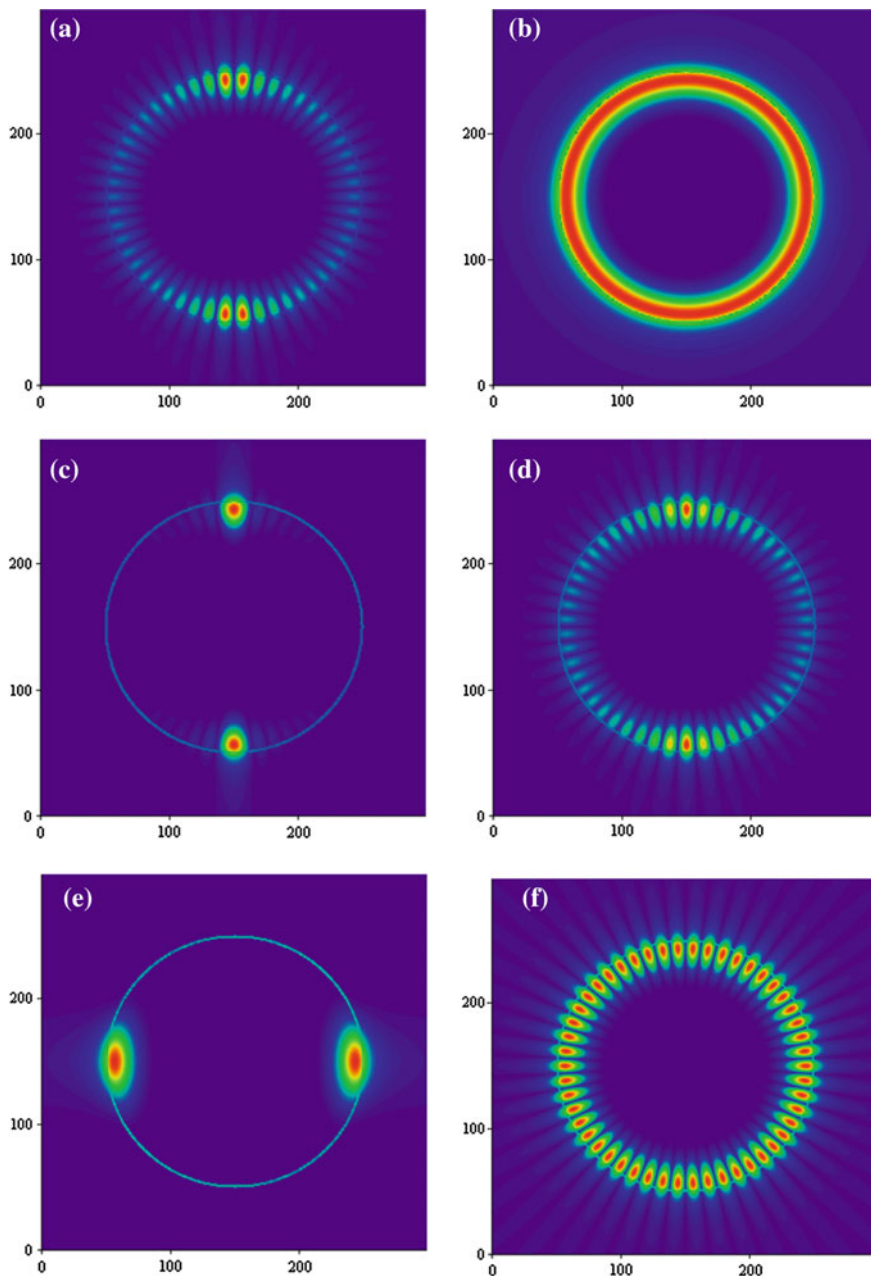


Fig. A.3 Module of the electric field distribution in the Spherical DR ($\epsilon_{1r} = 2, 2$) for the whispering gallery mode: $H_{25,0,1}$ (a, b); $H_{25,1,1}$ (c, d); $H_{25,25,1}$ (e, f)

not exist. The solution to the Maxwell's equations on the piecewise-smooth boundary of the Cylindrical DR is impossible to represent in so-called single-wave approximation as for Spherical DR (A.1.1).

In cases when the dielectric permittivity of DR is sufficiently large ($\varepsilon_{1r} = \varepsilon_1/\varepsilon_0 \gg 1$), the eigenmode field inside resonator can be sufficiently described by solutions to the Maxwell's equations obtained in the cylindrical coordinate system. Meanwhile, usually one or several boundary conditions on the external angular surface cannot be satisfied. However, in view of high Q of oscillations, the field in the external area small and frequency calculation error usually does not exceed 5–8 %. By utilizing the approximate representation inside the dielectric the sufficiently accurate computation of all DR parameters can be achieved.

Let us denote by L and r_0 the height and radius of the cylinder correspondingly (Fig. A.1b). The eigenoscillation field inside DR can be generally presented in the form of a standing wave in the circular dielectric waveguide described in the cylindrical coordinate system (ρ, α, z) :

$$\begin{aligned}
 e_\rho &= \left[e_1 \frac{\beta_z}{\beta} J'_m(\beta\rho) + h_1 m \frac{i\omega\mu_0}{\beta} \cdot \frac{J_m(\beta\rho)}{\beta\rho} \right] \begin{Bmatrix} \sin m\alpha \\ \cos m\alpha \end{Bmatrix} \begin{bmatrix} \cos \beta_z z \\ -\sin \beta_z z \end{bmatrix}; \\
 e_\alpha &= \left[e_1 m \frac{\beta_z}{\beta} \cdot \frac{J_m(\beta\rho)}{\beta\rho} + h_1 \frac{i\omega\mu_0}{\beta} \cdot J'_m(\beta\rho) \right] \begin{Bmatrix} \cos m\alpha \\ -\sin m\alpha \end{Bmatrix} \begin{bmatrix} \cos \beta_z z \\ -\sin \beta_z z \end{bmatrix}; \\
 e_z &= e_1 J_m(\beta\rho) \begin{Bmatrix} \sin m\alpha \\ \cos m\alpha \end{Bmatrix} \begin{bmatrix} \sin \beta_z z \\ \cos \beta_z z \end{bmatrix}; \\
 h_\rho &= \left[e_1 m \frac{i\omega\varepsilon_1}{\beta} \cdot \frac{J_m(\beta\rho)}{\beta\rho} - h_1 \frac{\beta_z}{\beta} \cdot J'_m(\beta\rho) \right] \begin{Bmatrix} \cos m\alpha \\ -\sin m\alpha \end{Bmatrix} \begin{bmatrix} \sin \beta_z z \\ \cos \beta_z z \end{bmatrix}; \\
 h_\alpha &= \left[-e_1 \frac{i\omega\varepsilon_1}{\beta} \cdot J'_m(\beta\rho) + h_1 m \frac{\beta_z}{\beta} \cdot \frac{J_m(\beta\rho)}{\beta\rho} \right] \begin{Bmatrix} \sin m\alpha \\ \cos m\alpha \end{Bmatrix} \begin{bmatrix} \sin \beta_z z \\ \cos \beta_z z \end{bmatrix}; \\
 h_z &= h_1 J_m(\beta\rho) \begin{Bmatrix} \cos m\alpha \\ -\sin m\alpha \end{Bmatrix} \begin{bmatrix} \cos \beta_z z \\ -\sin \beta_z z \end{bmatrix};
 \end{aligned} \tag{A.1.6}$$

where $J'_m(z)$ —is the derivative of the Bessel function of the first kind; e_1, h_1 —are the unknown amplitudes of the electrical and magnetic field inside resonator; β, β_z —are the wave numbers. The constants e_1, h_1 and β, β_z can be defined in different ways, depending on external DR field.

In order to obtain an approximate solution to the eigenoscillation task let us consider the external field representation as damped waves. In the area: $\rho > r_0$; $-L/2 \leq z \leq L/2$ the field can be represented proportionally to the modified Bessel function of the second kind: $K_m(\beta_0\rho)$; in the area: $\rho \leq r_0$; $|z| \geq L/2$ the DR field will have the form (A.1.6), i.e., in the z -axes behave as exponentially decreasing function $\exp(-\beta_{0z}|z|)$. Herewith, the constants $\beta, \beta_z; \beta_0, \beta_{0z}$ should satisfy conditions:

$$\beta^2 + \beta_z^2 = k_1^2; \quad -\beta_0^2 + \beta_z^2 = k_0^2; \quad \beta^2 - \beta_0^2 = k_0^2; \quad (\text{A.1.7})$$

The continuity condition of the field tangent components on the DR surface leads to the combined equations with unknown amplitudes e_0, h_0, e_1, h_1 . By accounting for nontrivial solution of the equations system the following relations for the characteristic parameters can be obtained:

$$\begin{aligned} & \left[\frac{\varepsilon_{1r} J'_m(\beta r_0)}{\beta J_m(\beta r_0)} + \frac{1}{\beta_0 r_0} \frac{K'_m(\beta_0 r_0)}{K_m(\beta_0 r_0)} \right] \cdot \left[\frac{1 J'_m(\beta r_0)}{\beta J_m(\beta r_0)} + \frac{1}{\beta_0} \frac{K'_m(\beta_0 r_0)}{K_m(\beta_0 r_0)} \right] \\ & = \left(\frac{m\beta_z}{k_0 r_0} \right)^2 \left(\frac{1}{\beta^2} + \frac{1}{\beta_0^2} \right)^2. \end{aligned} \quad (\text{A.1.8})$$

By approximately meeting the boundary requirements on the surfaces: $z = \pm L/2$, one obtains

$$\beta_{0z} = \beta_z \cdot \begin{bmatrix} -ctg\beta_z L/2 \\ tg\beta_z L/2 \end{bmatrix} \quad (\text{A.1.9})$$

for the mode HE_{nml}^\mp ;

$$\varepsilon_{1r} \beta_{0z} = \beta_z \cdot \begin{bmatrix} tg\beta_z L/2 \\ -ctg\beta_z L/2 \end{bmatrix} \quad (\text{A.1.10})$$

for the mode EH_{nml}^\pm .

Hence, the solution for amplitudes has the form

$$e_1 = a_0 \frac{m\beta_z}{r_0} \left(\frac{1}{\beta^2} + \frac{1}{\beta_0^2} \right); \quad h_1 = a_0 \left[\frac{i\omega\varepsilon_1 J'_m(\beta r_0)}{\beta J_m(\beta r_0)} + \frac{i\omega\varepsilon_0 K'_m(\beta_0 r_0)}{\beta_0 K_m(\beta_0 r_0)} \right].$$

In practice, the normalized amplitudes are suitably used proportional to

$$e_0 = \frac{\beta_z}{\beta} e_1; \quad h_0 = -i \frac{\omega\mu_0}{\beta} h_1,$$

and satisfy the relationships

$$h_0 + e_0 = \frac{J_{m-1}(p_\perp)}{p_\perp J_m(p_\perp)} - \frac{K_{m-1}(p_{0\perp})}{p_{0\perp} K_m(p_{0\perp})}; \quad h_0 - e_0 = \frac{J_{m+1}(p_\perp)}{p_\perp J_m(p_\perp)} + \frac{K_{m+1}(p_{0\perp})}{p_{0\perp} K_m(p_{0\perp})}. \quad (\text{A.1.11})$$

Here and below $p_\perp = \beta r_0$; $p_{0\perp} = \beta_0 r_0$. Equation (A.1.8) can be divided into two parts:

$$\begin{aligned} \frac{J'_m(\beta r_0)}{m\beta r_0 J_m(\beta r_0)} &= -\frac{1}{2} \left(\frac{1}{\varepsilon_{1r}} + 1 \right) \frac{K'_m(\beta_0 r_0)}{m\beta_0 r_0 K_m(\beta_0 r_0)} \\ &\pm \left\{ \frac{1}{4} \left(\frac{1}{\varepsilon_{1r}} - 1 \right)^2 \left[\frac{K'_m(\beta_0 r_0)}{m\beta_0 r_0 K_m(\beta_0 r_0)} \right]^2 + \frac{1}{\varepsilon_{1r}} \left(\frac{\beta_z}{k_0 r_0^2} \right)^2 \left(\frac{1}{\beta^2} + \frac{1}{\beta_z^2} \right)^2 \right\}^{1/2}, \end{aligned} \quad (\text{A.1.12})$$

assorted to the EH_{nml}^\mp (sign + in the (A.1.12)) and HE_{nml}^\pm (sign - in the (A.1.12)) oscillations.

Equation (A.1.12) is solved jointly with (A.1.7), (A.1.9), or (A.1.10).

In the cases of low dielectric permittivity the most suitable solution representation in the DR external region should be proportional to the Hankel function of the second kind [2] $H_m^{(2)}(\beta_0 \rho)$. In order to obtain the real characteristic parameters, usually the following relations have been assumed: $H_m^{(2)}(\beta_0 \rho) \approx Y_m(\beta_0 \rho)$. Here the functions $K_m(\beta_0 r_0)$ in (A.1.12) should be formally substituted by $Y_m(\beta_0 r_0)$, and Equations (A.1.7) should be changed to

$$\beta^2 + \beta_z^2 = k_1^2; \quad \beta_0^2 + \beta_z^2 = k_0^2; \quad \beta^2 - \beta_{0z}^2 = k_0^2. \quad (\text{A.1.13})$$

The amplitudes (A.1.11) are also exchanged onto

$$h_0 + e_0 = \frac{J_{m-1}(p_\perp)}{p_\perp J_m(p_\perp)} + \frac{Y_{m-1}(p_{0\perp})}{p_{0\perp} Y_m(p_{0\perp})}, \quad h_0 - e_0 = \frac{J_{m+1}(p_\perp)}{p_\perp J_m(p_\perp)} + \frac{Y_{m+1}(p_{0\perp})}{p_{0\perp} Y_m(p_{0\perp})}. \quad (\text{A.1.14})$$

In case of the azimuthally symmetric oscillations ($m = 0$) (A.1.12) is decomposed on two independent:

$$\frac{1}{\beta} \cdot \frac{J_1(\beta r_0)}{J_0(\beta r_0)} + \frac{1}{\beta_0} \cdot \frac{K_1(\beta_0 r_0)}{K_0(\beta_0 r_0)} = 0, \quad (\text{A.1.15})$$

corresponding to the magnetic modes: H_{n0l}^\pm ;

$$\frac{\varepsilon_{1r}}{\beta} \cdot \frac{J_1(\beta r_0)}{J_0(\beta r_0)} + \frac{1}{\beta_0} \cdot \frac{K_1(\beta_0 r_0)}{K_0(\beta_0 r_0)} = 0, \quad (\text{A.1.16})$$

corresponding to the electrical modes E_{n0l}^\mp .

In the literature the H_{101}^+ is known as $TE_{01\delta}$ or $H_{01\delta}$ mode, and the E_{101}^+ is known as $TH_{01\delta}$, or $E_{01\delta}$ mode [1].

The unknown field components are obtained from (A.1.6) by formally setting $e_1 = 0$ for magnetic modes: H_{n0l}^\pm and $h_1 = 0$ for electrical modes E_{n0l}^\mp .

For example, for H_{101}^+ mode, inside the dielectric area $\rho \leq r_0$; $|z| \leq L/2$ the following relations can be obtained:

$$\begin{aligned}
e_\rho &= e_z = h_\alpha = 0; \\
e_\alpha &= h_1 \frac{i\omega\mu_0}{\beta} \cdot J'_0(\beta\rho) \cdot \cos \beta_z z; \\
h_\rho &= -h_1 \frac{\beta_z}{\beta} \cdot J'_m(\beta\rho) \cdot \sin \beta_z z; \\
h_z &= h_1 J_0(\beta\rho) \cos \beta_z z.
\end{aligned} \tag{A.1.17}$$

However, the derived approximate field representation is not defined in the angular area: $\rho \geq r_0$; $|z| \geq L/2$ and, also do not satisfy the radiation conditions. The exterior DR field can be approximately calculated if we know the field inside resonator. By applying the known field expansions for the Cylindrical DR in the circular metal waveguide [3], the approximate solutions for the exterior DR field can be obtained. The simplest way of the necessary relations obtainment is by using the field decomposition of DR coaxially disposed in the circular metal waveguide (Fig. A.1c). For the H_{101}^+ mode with $|z| \geq L/2$ the field can be represented in the form

$$\begin{pmatrix} e_\rho \\ e_\alpha \\ e_z \end{pmatrix} = \sum_{s=1}^{\infty} c_{s0}^{\pm} \begin{pmatrix} 0 \\ E_\alpha^{s0\pm} \\ 0 \end{pmatrix}; \quad \begin{pmatrix} h_\rho \\ h_\alpha \\ h_z \end{pmatrix} = \sum_{s=1}^{\infty} c_{s0}^{\pm} \begin{pmatrix} H_\rho^{s0\pm} \\ 0 \\ H_z^{s0\pm} \end{pmatrix}, \tag{A.1.18}$$

where $E_\alpha^{s0\pm}$, $H_\rho^{s0\pm}$, $H_z^{s0\pm}$ —are the α , ρ and z components of the electrical and magnetic field of the azimuthally symmetric waves of the circular waveguide, respectively; c_{s0}^{\pm} —are the decomposition coefficients in the area: $z \geq L/2$ —sign “+” and $z \leq -L/2$ —sign “-” [3]. All components of the decomposition (A.1.18) are the functions on the DR parameters and waveguide radius R .

In order to derive the desired eigenmodes of Cylindrical DR in the Open space, let us approach to the limit $R \rightarrow \infty$ in (A.1.18). By taking into account that the sum on s will be transformed into integral, the nonzero components after simple transformations will take the form

$$\begin{aligned}
e_\alpha &= w_0 r_0 h_1 \frac{(k_1^2 - k_0^2)}{\beta} \int_0^\infty \varphi(\eta) \cdot J_1(\eta k_0 \rho) \cdot e^{\mp i\gamma k_0 z} \cdot \frac{\eta d\eta}{|\gamma|}; \\
h_\rho &= \mp r_0 h_1 \frac{(k_1^2 - k_0^2)}{\beta} \int_0^\infty \varphi(\eta) \cdot J_1(\eta k_0 \rho) \cdot e^{\mp i\gamma k_0 z} \cdot \eta d\eta; \\
h_z &= i r_0 h_1 \frac{(k_1^2 - k_0^2)}{\beta} \int_0^\infty \varphi(\eta) \cdot J_0(\eta k_0 \rho) \cdot e^{\mp i\gamma k_0 z} \cdot \frac{\eta^2 d\eta}{|\gamma|}.
\end{aligned} \tag{A.1.19}$$

Here $\gamma = \sqrt{1 - \eta^2}$;

$$\varphi(\eta) = \frac{\left[\frac{p_{\perp}}{q_{\perp}} J_0(p_{\perp}) J_1(q_{\perp} \eta) - \eta J_1(p_{\perp}) J_0(q_{\perp} \eta) \right]}{\left[\left(\frac{p_{\perp}}{q_{\perp}} \right)^2 - \eta^2 \right]} \cdot \frac{\left[\frac{p_z}{q_z} \sin p_z \cos q_z \gamma - \gamma \cos p_z \sin q_z \gamma \right]}{\left(\frac{p_z}{q_z} \right)^2 - \gamma^2}, \quad (\text{A.1.20})$$

and $p_z = \beta_z L/2$; $q_{\perp} = k_0 r_0$; $q_z = k_0 L/2$.

The obtained relationships are rather cumbersome and too complicated, in addition they are valid only in the area $|z| \geq L/2$. A good approximation of integrals' calculation (A.1.19) can be achieved by

$$\varphi(\eta) \approx \varphi(1) \cdot \eta. \quad (\text{A.1.21})$$

By substituting (A.1.20) into (A.1.21) in (A.1.19) and using the integral (A.3.1), all cylindrical components of the DR field can be calculated in the spherical coordinate system (r, θ, φ) as

$$\begin{aligned} e_{\alpha} &\approx w_0 r_0 h_1 \frac{(k_1^2 - k_0^2)}{\beta} \varphi(1) \cdot \sin \theta \cdot h_1^{(2)}(k_0 r); \\ h_{\rho} &\approx i r_0 h_1 \frac{(k_1^2 - k_0^2)}{\beta} \varphi(1) \cdot \sin \theta \cos \theta \cdot \left[\frac{3}{k_0 r} h_1^{(2)}(k_0 r) - h_0^{(2)}(k_0 r) \right]; \\ h_z &\approx i r_0 h_1 \frac{(k_1^2 - k_0^2)}{\beta} \varphi(1) \cdot \left[\sin^2 \theta \cdot h_0^{(2)}(k_0 r) + \frac{2 \cos^2 \theta - \sin^2 \theta}{k_0 r} \cdot h_1^{(2)}(k_0 r) \right]. \end{aligned} \quad (\text{A.1.22})$$

Consequently, the obtained expressions turn out to be proportional to the corresponding field components of the Spherical DR in H_{101} mode. At some distance from the Cylindrical DR the field of H_{101}^+ mode becomes similar to the field of the main magnetic mode H_{101} of the Spherical DR.

Figure A.4 shows the comparative calculations of the E-field, obtained with the help of (A.1.19), (A.1.20), and (A.1.22). As it can be clearly seen, the visible difference between field distributions can be observed only near angular area of the cylinder. Herewith, (A.1.22) gives good approximation in the area $r \geq \sqrt{(L/2)^2 + r_0^2}$.

In the distant region the field of the Cylindrical DR in H_{101}^+ mode, calculated on the basis of the Kirchhoff's theorem is also proportional to the function (A.1.20) [P.3]:

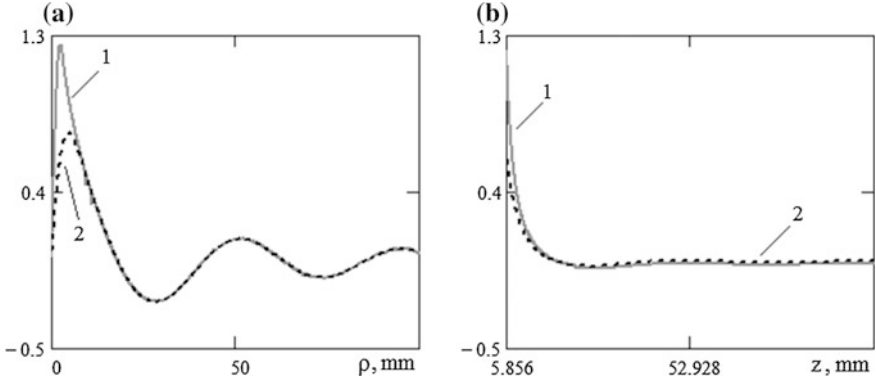


Fig. A.4 The $\text{Re}(e_\alpha)$ response of the cylindrical DR at the frequency 7 GHz with $\varepsilon_{1r} = 36$, $\Delta = L/2r_0 = 2$, calculated according to (A.1.19)—marked by *continuous curves*; (A.1.22) by *dotted curves*; $z = L/2$ (a), $\rho = r_0$ (b)

$$e_\theta = e_r = 0;$$

$$e_\alpha = \frac{e^{-ik_0 r}}{r} \cdot h_0 r_0 (\varepsilon_{1r} - 1) \cdot \varphi(\sin \theta), \quad h_\theta = -e_\alpha / w_0. \quad (\text{A.1.23})$$

The energy, stored in the DR material, $w = 1/4 \int_{V_p} \left(\varepsilon_1 |\vec{e}_1|^2 + \mu_0 |\vec{h}_1|^2 \right) dv$ on the frequency of the main mode H_{101}^+ is

$$\begin{aligned} w &= \frac{\pi r_0^2 \varepsilon_1 w_0^2}{8 \beta_z} |h_1|^2 \\ &\cdot \left[\left\{ \left(\frac{k_0}{\beta} \right)^2 [J_1^2(p_\perp) - J_0(p_\perp) J_2(p_\perp)] + \frac{1}{\varepsilon_{1r}} [J_0^2(p_\perp) + J_1^2(p_\perp)] \right\} (2p_z + \sin 2p_z) \right. \\ &\left. + \frac{1}{\varepsilon_{1r}} \left(\frac{\beta_z}{\beta} \right)^2 [J_1^2(p_\perp) - J_0(p_\perp) J_2(p_\perp)] (2p_z - \sin 2p_z) \right] \approx \frac{\pi q_\perp^2 \varepsilon_1 w_0^2}{4 \beta^2 \beta_z} |h_1|^2 \cdot v_0 \end{aligned} \quad (\text{A.1.24})$$

here

$$v_0 = [J_1^2(p_\perp) - J_0(p_\perp) J_2(p_\perp)] (2p_z + \sin 2p_z). \quad (\text{A.1.25})$$

In the common cases of the EH_{nml}^\pm or HE_{nml}^\mp modes:

$$w = \frac{\pi r_0^2 \varepsilon_1}{32 \beta_z} (1 + \delta_{m0}) \cdot w_{nml},$$

where

$$\begin{aligned}
 w_{nml} = & \left[(e_0 - h_0)^2 \left[J_{m-1}^2(p_\perp) - J_m(p_\perp)J_{m-2}(p_\perp) \right] + (e_0 + h_0)^2 \left[J_{m+1}^2(p_\perp) - J_m(p_\perp)J_{m+2}(p_\perp) \right] \right. \\
 & \left. + 2 \left(\frac{\beta}{k_1} h_0 \right)^2 \left[J_m^2(p_\perp) - J_{m-1}(p_\perp)J_{m+1}(p_\perp) \right] \right] \begin{bmatrix} 2p_z + \sin 2p_z \\ 2p_z - \sin 2p_z \end{bmatrix} \\
 & + \left[\left(\frac{k_1}{\beta_z} e_0 - \frac{\beta_z}{k_1} h_0 \right)^2 \left[J_{m-1}^2(p_\perp) - J_m(p_\perp)J_{m-2}(p_\perp) \right] \right. \\
 & \left. + \left(\frac{k_1}{\beta_z} e_0 + \frac{\beta_z}{k_1} h_0 \right)^2 \left[J_{m+1}^2(p_\perp) - J_m(p_\perp)J_{m+2}(p_\perp) \right] \right. \\
 & \left. + 2 \left(\frac{\beta}{\beta_z} e_0 \right)^2 \left[J_m^2(p_\perp) - J_{m-1}(p_\perp)J_{m+1}(p_\perp) \right] \right] \begin{bmatrix} 2p_z - \sin 2p_z \\ 2p_z + \sin 2p_z \end{bmatrix}.
 \end{aligned}
 \tag{A.1.26}$$

References

1. D. Kajfez, P. Guillon. *Dielectric Resonators* (Noble Publishing Corporation, Atlanta, 1998)
2. Handbook of mathematical functions. Eds. by M. Abramowitz and I. Stegun (National bureau of standards, 1964)
3. M.E. Ilchenko, A.A. Trubin, *Electrodynamics of Dielectric Resonators* (Kiev, Naukova Dumka, 2004)
4. A.A. Trubin, *Several Specified Integrals of Special Functions* (EqWorld, 06.02.2010), <http://eqworld.ipmnet.ru/ru/auxiliary/aux-specfunc.htm>

Appendix 2

Perturbation Theory for the Maxwell's Equations

The Maxwell's equations with the fields that vary with time as $\vec{E} = \vec{E}_m e^{i\omega t}$; $\vec{H} = \vec{H}_m e^{i\omega t}$ can be presented in the form

$$\text{rot}\vec{H} = i\tilde{\omega}\varepsilon\vec{E}, \quad \text{rot}\vec{E} = -i\tilde{\omega}\mu\vec{H}. \tag{A.2.1}$$

In the general case suppose that a circular frequency $\tilde{\omega} = \omega' + i\omega''$ and the dielectric permittivity $\varepsilon = \varepsilon' - i\varepsilon''$ are the complex, and magnetic permeability is real $\mu = \mu_0$.

In the majority cases the practically applied dielectrics are described by sufficiently high values of the relative dielectric permittivity: $\varepsilon'/\varepsilon_0 \gg 1$, and small dissipative losses: $\varepsilon''/\varepsilon' \ll 1$. Here ε_0 —is the dielectric permittivity of the vacuum. In the cases of high-Q resonators one can establish an assumption $\omega'' \ll \omega'$.

Let us suppose that we have two different solutions to the same boundary problem of Maxwell's equations (A.2.1), namely: the (\vec{E}_1, \vec{H}_1) , with complex frequency $\tilde{\omega}_1$ and the (\vec{E}_2, \vec{H}_2) with complex frequency $\tilde{\omega}_2$. Let us substitute each of the solutions in (A.2.1) by using the known vector equation:

$$\text{div}[\vec{F}, \vec{G}] = (\vec{G}, \text{rot}\vec{F}) - (\vec{F}, \text{rot}\vec{G}).$$

Thus, we obtain

$$\text{div}\{[\vec{E}_1, \vec{H}_2^*] + [\vec{E}_2^*, \vec{H}_1]\} = i(\tilde{\omega}_2^* - \tilde{\omega}_1)[\varepsilon'(\vec{E}_1, \vec{E}_2^*) + \mu_0(\vec{H}_1, \vec{H}_2^*)] - \varepsilon''(\tilde{\omega}_1 + \tilde{\omega}_2^*)(\vec{E}_1, \vec{E}_2^*). \tag{A.2.2}$$

By denoting the last one as $\omega_0 = (\omega'_1 + \omega'_2)/2$, the corresponding relation (A.2.2) can be rewritten in the form

$$\frac{1}{\omega_0} \text{div}\{[\vec{E}_1, \vec{H}_2^*] + [\vec{E}_2^*, \vec{H}_1]\} = i \frac{(\tilde{\omega}_2^* - \tilde{\omega}_1)}{\omega_0} [\varepsilon'(\vec{E}_1, \vec{E}_2^*) + \mu_0(\vec{H}_1, \vec{H}_2^*)] - \varepsilon'' \frac{\tilde{\omega}_1 + \tilde{\omega}_2^*}{\omega_0} (\vec{E}_1, \vec{E}_2^*). \tag{A.2.3}$$

If the field (\vec{E}_1, \vec{H}_1) does not strongly differ from the (\vec{E}_2, \vec{H}_2) , then the parameter $\xi = (\tilde{\omega}_2^* - \tilde{\omega}_1)/\omega_0$ is small in absolute value: $|\xi| \ll 1$ and the obtained expression can be applied as the basic one in perturbation theory.

In some cases it is more convenient to search the solution when the dielectric losses are absent: $\varepsilon'' = 0$. Consequently, (A.2.3) becomes simpler:

$$\frac{1}{\omega_0} \operatorname{div}\{[\vec{E}_1, \vec{H}_2^*] + [\vec{E}_2^*, \vec{H}_1]\} = i \frac{(\tilde{\omega}_2^* - \tilde{\omega}_1)}{\omega_0} [\varepsilon'(\vec{E}_1, \vec{E}_2^*) + \mu_0(\vec{H}_1, \vec{H}_2^*)]. \quad (\text{A.2.4})$$

Appendix 3

Certain Integral Relations for Special Functions

The below given integrals allow to obtain analytical relationships for the field and DR coupling coefficients in the transmission line as well as in the Open space.

The integral [4]

$$\int_0^\infty e^{-ib\sqrt{1-t^2}} J_m(ct) P_n^m(\sqrt{1-t^2}) t dt / \sqrt{1-t^2} = i^{(m-n)} P_n^m\left(b/\sqrt{b^2+c^2}\right) h_n^{(2)}\left(\sqrt{b^2+c^2}\right). \tag{A.3.1}$$

Here b, c —are the real constants; $h_n^{(2)}(z)$ —is the spherical Hankel function of the second kind [2]. Proof of (A.3.1) is carried out by induction method and follow from recurrence relations for the associated Legendre polynomials and cylindrical functions [2].

In the particular case: $n = m = 0$ the expression (A.3.1) obtains a simpler form, known as Sommerfeld’s integral:

$$\int_0^\infty e^{-ib\sqrt{1-t^2}} J_0(ct) t dt / \sqrt{1-t^2} = h_0^{(2)}\left(\sqrt{b^2+c^2}\right). \tag{A.3.2}$$

By differentiating (A.3.2) m times on the parameter b , we obtain

$$\int_0^\infty (\sqrt{1-t^2})^m J_0(ct) e^{-ib\sqrt{1-t^2}} t dt / \sqrt{1-t^2} = i^m \frac{d^m}{db^m} h_0^{(2)}\left(\sqrt{b^2+c^2}\right), \quad b > 0 \tag{A.3.3}$$

From which by using the expansion

$$t^{2m} = \sum_{s=0}^m (-1)^s \frac{m!}{(m-s)!s!} (\sqrt{1-t^2})^{2s}$$

it is possible to find one more useful integral:

$$\int_0^{\infty} t^{2m} J_0(ct) e^{-ib\sqrt{1-t^2}} t dt / \sqrt{1-t^2} = \sum_{s=0}^m \frac{m!}{(m-s)!s!} \cdot \frac{\partial^{2s}}{\partial b^{2s}} h_0^{(2)}(\sqrt{b^2+c^2}). \quad (\text{A.3.4})$$

The integral convergence (A.3.1)–(A.3.4), in the area $t \geq 1$ is provided by proper choice of the radical sign $-i\sqrt{t^2-1}$ in the exponent index.

According to (A.3.3) by approaching the limit $b = 0$ for the $m = 2n$ one obtains

$$\lim_{b \rightarrow 0} \int_0^{\infty} (\sqrt{1-t^2})^{2n} J_0(ct) e^{-ib\sqrt{1-t^2}} t dt / \sqrt{1-t^2} = (-1)^n \frac{d^{2n}}{db^{2n}} h_0^{(2)}(\sqrt{b^2+c^2}) \Big|_{b=0}. \quad (\text{A.3.5})$$

By putting $c = 0$ in (A.3.3) the following expression can be derived:

$$\int_0^{\infty} t^{2m} e^{-ib\sqrt{1-t^2}} t dt / \sqrt{1-t^2} = \sum_{s=0}^m \frac{m!}{(m-s)!s!} \cdot \frac{d^{2s}}{db^{2s}} h_0^{(2)}(b). \quad (\text{A.3.6})$$

Expressions (A.3.5) and (A.3.6) are not always suitable for calculation as they contain derivatives of higher degree. In the cases of $m \gg 1$, the derivatives can be simply calculated with the help of the decompositions:

$$\frac{d^n}{db^n} h_0^{(2)}(b) = h_0^{(2)}(b) \cdot n! \sum_{s=0}^n \frac{(-i)^{n+s}}{(n-s)!} \cdot \frac{1}{b^s}, \quad (\text{A.3.7})$$

and

$$\frac{d^{2n}}{db^{2n}} h_0^{(2)}(\sqrt{b^2+c^2}) \Big|_{b=0} = (-1)^n \cdot (2n)! \sum_{s=0}^n \frac{(4s+1)(2s)!}{2^{n+s}(n-s)!(s!)^2} \cdot \frac{1}{\prod_{u=0}^{n+s} (2u+1)} h_{2s}^{(2)}(c). \quad (\text{A.3.8})$$

The relation (A.3.7) arises from the spherical Hankel function representation via elementary functions as well as the Leibnitz theorem on product differencing. The decomposition (A.3.8) follows from the summation theorem for the spherical Hankel functions.

Index

A

Active DR, 99–101, 103, 104, 107, 112–115
Amplitude response, 17
Angle lattice, 91
Antenna, 1, 88, 97, 99, 102, 104, 105, 113, 145–147
Antiphased amplitude distribution, 17
Antiphased modes, 8, 9, 43
Aperture, 1, 79, 100, 104, 108, 109

B

Bandpass DR filter, 2, 47, 51, 53, 55, 61
Bandpass filter on laterally coupled disk microresonators, 72
Bandpass filter on ring microresonators, 70
Bandpass filter on spherical microresonators, 57
Bandpass filter on vertically coupled disk microresonators, 73
Band-stop DR filter, 47
Band-stop filter cascade connections, 72, 76
Bandstop filters on laterally coupled disk microresonators, 74
Bandstop filters on laterally coupled ring microresonators, 76
Bandstop filters on laterally coupled spherical microresonators, 74
Band-stop filters on spherical microparticles, 64, 66
Bouncing ball mode, 31

C

Causality conditions, 119
Chaotic oscillations, 17
Characteristic equation, 28–31
Chirp, 122, 124, 136

Completely cophased amplitude distribution, 21
Complex amplitude distribution, 16
Cophased, 7–9, 21, 97
Coupled oscillations, 5, 7, 13, 16, 17, 21, 24
Coupling coefficient, 7, 9, 10, 12, 13, 33, 39, 41, 53, 66, 70, 73, 100, 101, 105, 113
Coupling operator, 6, 49, 53
Coupling oscillation parameters, 17
Cross-section, 13, 17, 18, 57, 59, 61, 62, 101
Cylindrical DR, 1, 9, 12, 13, 24, 51, 55, 58, 60, 81, 82, 87, 89, 92, 94, 99
Cylindrical DR ring structure, 24

D

Dielectric resonators, 1, 5, 19, 23, 47, 79, 80, 97, 111
Dielectric waveguide, 66, 69–71
Differential scattering cross-section, 84
Distinguishing, 1, 113, 137
Double-band bandstop filter, 59
Double harmonic dependence, 19
DR eigenmodes, 68, 81
DR radiating element, 97, 99
DRs with different relative dimensions, 58
Dual-band dielectric filter, 59
Dual-band pass filter, 62

E

Eigenvalue problem, 6
Electromagnetic pulse, 117, 138, 145
Envelop, 62, 122, 123, 125, 126, 128, 129, 141, 148
Equivalent refractive index, 93, 95
Evanescent waveguide, 53–56, 58, 117
Even–even coupling mode, 34, 37, 38

- Even–odd mode, 34
- Excitation element, 99
- Expansion coefficient, 6, 10, 49, 100
- Exponential, 103, 131
- F**
- Far-field antenna radiation pattern, 104
- Far-field region, 91, 139, 145
- Feeding transmission line, 100, 145
- Field distribution, 6–8, 31, 38, 68, 98
- Forbidden zone, 26, 30, 31
- Forced DR oscillations, 108
- Frequency, 1, 5, 6, 17, 23, 24, 27, 44, 49, 54, 55, 60–63, 66, 74, 75, 79, 83, 92, 101, 116, 122, 125, 129, 133, 134
- Frequency gap, 19, 24
- Frequency response, 51, 54, 63, 70, 75, 111, 118, 121
- G**
- Gaussian, 122, 124–127, 137
- Green’s function of the bandpass filter, 119, 120
- Green’s functions for multiple bandstop filters, 120, 121, 129, 135
- Green’s functions of the one-layer DR lattice, 140
- Green’s functions of the Yagi-Uda antenna, 146
- Group delay, 54, 55, 57, 61, 69, 128
- Group velocity, 54, 56, 57, 65
- H**
- Hexagonal lattice of ring DRs, 44
- High Q oscillation, 17–19, 33
- I**
- Incidence and observation directions, 82
- Incident wave, 49, 80–83, 86–88, 91–93, 142
- Infrared wavelength range, 5, 30, 32, 64, 84
- Integral transformation, 10, 12
- L**
- Laterally coupled disk DRs, 38
- Lattice, 1, 6, 16–19, 21, 23, 24, 30, 31, 42–44, 47–49, 59–61, 64, 75, 79, 81–84, 86–89, 91–93, 104, 112–114
- Linear antenna grid, 100
- Linear cylindrical DR antenna lattice, 102, 103
- Linear lattice, 19, 64, 66, 69, 100, 121, 146
- Linear traveling-wave DR antenna, 105
- Localized oscillation, 18, 20, 23, 24
- Loop, 100, 101, 113
- Lorentzian, 131, 132, 136
- Lowest magnetic mode, 13
- Low Q oscillation, 19, 42
- M**
- Main antenna lobe, 104
- Meta-material, 93
- Microstrip line, 100
- Millimeter, 1, 2, 30, 32, 47, 97
- Multilayer lattice, 32
- Multilayer spherical dielectric lattice, 26
- Mutual coupling coefficient, 7, 10–15, 17, 32, 36, 76, 107
- Mutual influence of the pulses, 137
- N**
- Near-field region, 36, 87, 92
- O**
- Odd–even mode, 7, 8, 34, 37, 38
- Odd–odd mode, 37
- One-dimensional, 16, 18, 19, 23, 26, 30, 64, 97, 147
- One-dimensional antenna lattice, 99
- One-dimensional periodic structure, 26
- One-dimensional structure, 16
- Open space, 1, 2, 10, 12–14, 19–21, 24, 27, 28, 30, 68, 79, 81, 83, 93, 100, 102, 104, 107, 113, 117, 138, 143
- Optical microresonator, 32
- P**
- Parabolic DR antennas, 149
- Parabolic lattice, 86, 87
- Paraboloidal DR antenna, 114, 115
- Parallel-plate metal waveguide, 10–13, 66
- Parity, 35, 36, 39
- Passive DR, 106, 109, 111
- Perturbation theory, 6, 16, 64
- Photonic crystal, 5, 26, 30, 31
- Planar antenna, 113, 146
- Planar reflecting antenna, 112
- Plane wave scattering, 80, 86
- Power flux density, 83–85, 87, 89–91, 93, 98, 114
- P-polarization, 81
- Pulses radiation, 145

Q

Quality factor, 5, 7, 9, 16, 31, 120
 Quasi-optical band filter, 64

R

Rectangular, 1, 10, 12, 13, 16, 18, 24, 51, 55, 59, 62, 64, 80, 82, 87, 92, 108, 126, 133, 136, 137, 142, 143
 Rectangular waveguide, 10, 12, 13, 16–18, 23, 55, 56, 58, 59, 62, 63, 107–110
 Reflected lobe, 84
 Reflected wave, 79, 83, 121, 141
 Reflection coefficient, 49, 50, 53, 54, 60, 72, 101–104, 109, 110, 112–114, 118, 134
 Refracted lobe, 84
 Ring antenna, 106
 Ring antenna lattice, 106
 Ring DR, 42, 109
 Ring lattice, 21, 22, 25, 66, 67, 106
 Ring structure of ring DRs, 43

S

Scattering amplitude, 82, 139
 Scattering matrix, 51, 117
 Scattering of the pulses, 121
 Scattering theory, 47, 79
 Screening lattice, 23
 Shady lobe, 83, 87, 92
 Sinc, 130, 132, 136
 Single-layer plane square lattice, 81
 Single-resonator antenna, 97
 Slot line, 100
 S-matrix pole distribution, 120
 Snell's laws, 83, 86, 93
 Solitary mode, 19
 Soliton-like, 122, 123, 130, 132, 134, 136, 143, 144, 148
 Spectral rarefaction, 21
 Spherical cavity, 26, 30, 31, 33
 Spherical DR, 7, 8, 10, 12, 13, 19, 21, 24, 32, 36, 37, 57, 62, 98
 Spherical DR higher modes, 16, 17

Spherical microparticle, 64, 67
 Split cylindrical DR, 101, 102, 107, 108, 146
 S-polarization, 81, 140
 Square hexagonal lattice, 21
 Square lattice of ring DRs, 43
 Super-Gaussian, 123, 131, 133, 143, 145, 147
 Symmetry plane, 7, 16, 34, 36, 53, 91

T

Tetrahedral oblique prism lattice, 92–95, 143
 Three-dimensional antenna lattice, 97, 111
 Three-dimensional DR structure, 86, 89
 Three-edged prism lattice, 92
 Three-layered rectangular lattice, 95
 Time delay, 121, 128
 Time-domain Green's function, 117, 118, 121, 128
 Transmission band, 54, 66, 123, 128
 Transmission coefficient, 49, 53, 60, 61, 63, 64, 128, 138, 145
 Two-dimensional DR antenna lattice, 106
 Two-dimensional DR lattice, 21
 Two-layer spherical DR, 61, 62
 Two-layer square lattice, 89

U

Unidirectional scattering, 92

V

Vacancy, 18, 19, 22, 23, 63
 Various orientation DRs, 7, 59
 Vertically coupled disk DRs, 39

W

Wave zone, 82, 93, 98
 Whispering gallery mode, 5, 25, 32, 33, 37–40, 42, 43, 64, 68–71, 74, 121
 Wire element, 100

Y

Yagi-Uda cylindrical DR antenna, 104